APL Photonics

RESEARCH ARTICLE | OCTOBER 15 2025

Optical gain in O-band active regions with multiple dot-in-well layers

G. M. Jandu ; A. R. Smith ; C. P. Allford ; S. Power ; P. Mishra ; Z. Cao ; L. Jarvis ; X. Zhang ; H. Deng ; M. Tang ; H. Liu ; P. M. Smowton

APL Photonics 10, 106112 (2025)
https://doi.org/10.1063/5.0275039

Optical gain in O-band active regions with multiple dot-in-well layers

Cite as: APL Photon. 10, 106112 (2025); doi: 10.1063/5.0275039
Submitted: 10 April 2025 • Accepted: 1 October 2025 •
Published Online: 15 October 2025

G. M. Jandu,[1,a)] A. R. Smith,[1] C. P. Allford,[1] S. Power,[1] P. Mishra,[1] Z. Cao,[1] L. Jarvis,[1] X. Zhang,[2] H. Deng,[2] M. Tang,[2] H. Liu,[2] and P. M. Smowton[1]

AFFILIATIONS

[1] School of Physics and Astronomy, Cardiff University, The Parade, Cardiff CF24 3AA, United Kingdom
[2] Department of Electronic and Electrical Engineering, University College London, Torrington Place, London WC1E 7JE, United Kingdom

[a)] **Author to whom correspondence should be addressed:** JanduGM@cardiff.ac.uk

ABSTRACT

The optimum number of layers in InAs-based quantum dot-in-well active regions is investigated by means of sophisticated measurements of structures containing 8, 12, and 14 dot-in-well layers. Measurements of optical gain vs a parameter proportional to the carrier density indicate that additional layers do provide a proportional increase in the available gain at a given carrier density. This indicates that unequal optical overlap and unequal electrical pumping of the different layers are not significant effects. It is suggested that performance better than that of the typically used seven or eight layers may occur for samples with a higher layer number with reduced levels of p-modulation doping to minimize internal optical mode loss and non-radiative recombination.

I. INTRODUCTION

To meet rising data traffic demands driven by the increased use of artificial intelligence software and other data-intensive activities, fast, inexpensive, and versatile data transmission methods are required.[1] In particular, high-power, O-band, on-chip lasers are needed for edge processors and other data communication applications.[2]

Quantum dot-in-well (DWELL) active regions are attractive candidates for use in this regard due to their temperature insensitivity, resistance to optical feedback, and long device lifetimes.[2] InAs quantum dots (QDs) are suitable for uncooled lasing operation in the O-band, reducing device footprint and net power consumption. The highest operating temperature lasers on GaAs[3] and Si[4] substrates both use eight InAs/InGaAs DWELL layers with p-modulation doping (hereafter referred to as p-doping).

The number of stacked DWELL layers is a critical design parameter. Increasing the layer count reduces the gain requirement per dot; however, it can lead to an increase in the total current needed to pump enough dots to the required level. Consequently, in the same way that there is an optimal lasing cavity length,[5] there exists an optimal number of DWELL layers beyond which the gain no longer increases proportionally at a given carrier concentration. This optimum has been explicitly demonstrated for p-doped InAs/InP DWELL lasers;[6] however, it likely differs for InAs/InGaAs DWELL lasers.

A theoretical optimization accounting for these effects was first introduced for quantum well (QW) lasers by Ilroy *et al.*[7] However, for large numbers of layers, additional effects become significant. One such effect is impeded carrier transport across the intrinsic region, which leads to a higher population of holes near the p-side and electrons near the n-side, resulting in reduced gain, as reported in QW lasers.[8]

Another key factor is the overlap of the optical mode with the active region. A mode propagating through a waveguide with a thin active region is likely to have a poor confinement factor,[9] meaning that a significant portion of the mode does not experience gain. Conversely, overly thick active regions lead to inefficient pumping due to poor optical overlap with the outer layers.[10] Carefully engineered separate confinement heterostructure (SCH) layers can be used to increase the optical confinement factor of thin active regions (by changing the aluminum content, e.g., see Ref. 11); however, there are some benefits to using more layers.

When layers can be equally populated, increasing their number reduces the gain requirement per layer and, therefore, the carrier concentration at threshold. This reduces the likelihood of non-radiative recombination in the wetting layer, which is inefficient and can induce dislocation climb,[12] leading to areas of non-luminescence and device degradation.[13] Consequently, the design of efficient, long-lived devices requires an understanding of how optical gain scales with layer number.

For p-doped InAs/InGaAs DWELL lasers, seven or eight layers of dots have produced the best performance, including operation at the highest temperatures. However, recent work has demonstrated that co-doping, the combination of p-doping with n-type doping, has advantages over p-doping alone.[14] While both doping schemes reduce temperature sensitivity, p-doping significantly increases threshold current,[15] whereas co-doped lasers have demonstrated reduced thresholds compared to n-doped and undoped lasers.[16] It is not yet understood whether co-doped InAs/InGaAs lasers could benefit from more than eight DWELL layers.

The present work addresses this issue by comparing nominally identical structures with different numbers of DWELL layers. To assess the impact of layer number on carrier transport and optical overlap, we use the electrically pumped segmented contact method[17] (SCM) to measure the gain and absorption spectra of co-doped InAs/InGaAs DWELL active regions with 8, 12, and 14 DWELL layers. The analysis of these spectra reveals that, although the 14-layer sample shows some variation in dot distribution, gain continues to scale with layer number beyond the conventional 8-layer design. This suggests that neither unequal pumping nor poor optical overlap limits performance for the layer numbers investigated here.

Section II outlines the intended epitaxial structure and the growth methodology. Section III describes the measurement process. The final results are presented in Sec. IV.

II. EPITAXIAL GROWTH AND DEVICE STRUCTURE

The epitaxial layers of the wafers are shown schematically in Fig. 1. Each DWELL layer consists of 2.85 monolayers of InAs QDs in an $In_{0.16}Ga_{0.84}As$ QW followed by 35.5 nm of GaAs spacing layers that contain the Be p-dopants. The dots are grown via the Stranski–Krastanov (SK) growth mode[18] with silicon atoms introduced during the self-assembly process providing the n-dopants.

All layers were grown using a Veeco GEN 930 Molecular Beam Epitaxy system. The $In_{0.16}Ga_{0.84}As$ QW and InAs QDs were grown at a constant temperature of 510 °C with the Si shutter briefly opened during the QD growth, targeting a Si atom density of 780 μm^{-2} in each dot layer.[1] The GaAs spacing layers were grown in two temperature stages. Initially, 10.5 nm of GaAs was deposited at 510 °C; the temperature was kept low here to avoid diffusion of Ga into the QDs and to prevent deformation of the QD shape.[19] Keeping the temperature constant, the Be shutter was opened for the subsequent 10 nm of growth with the intention of obtaining a continuous p-type doping profile with a Be density of 650 000 μm^{-3}. The final 15 nm of GaAs was grown at 580 °C, acting as a high temperature growth spacer layer (HTGSL), which serves to replanarize the surface to minimize the impact of the non-planar dot surface on subsequent DWELL layers.[20]

The doping concentrations were calculated based on the dot density estimated from an atomic force microscopy (AFM) image of an uncapped calibration sample. The dot density was found to be 650 μm^{-2} per dot layer, meaning that the targeted doping densities correspond to 1.2 electrons per dot and 10 holes per dot. To avoid possible systematic changes in growth conditions impacting the results, the samples were grown in a pseudo-random order, with the 12-layer sample grown first, then the 14-layer sample, and finally the 8-layer sample. These were then fabricated into 50 μm wide oxide-isolated stripes with segmented contacts with section lengths of 150 μm.

Photoluminescence (PL) measurements were taken for each sample by illuminating a spot of material away from the metal contacts with a continuous wave HeNe laser at both low (207.7 W cm^{-2}) and high (2077 W cm^{-2}) power. The results of applying a Butterworth filter to the raw data (to remove high-frequency noise) are plotted in Fig. 2. The four peaks visible for the lower layer samples shown in Fig. 2(b) from left to right are identified as wetting layer emission, the second dot excited state (ES), the first ES, and the dot ground state (GS).

The emission peaks in the 14-layer sample are broadened, indicating a difference in dot distribution, which we attribute to an unintentional difference in growth conditions in this portion of the wafer. The distribution of SK quantum dots is highly sensitive to growth conditions such as surface roughness and temperature, which poses challenges for achieving uniformity in wafer-scale growth.[21] However, we note that the variation in dot distribution only has a minor impact on the outcomes of this study; although the rate of peak gain increase with carrier concentration is slightly reduced, the peak gain per layer remains in good agreement across all samples. There was also some variation in the GS peak position of the 14-layer sample across the wafer, indicating that further optimizations are required to preserve dot uniformity for thicker active regions. The

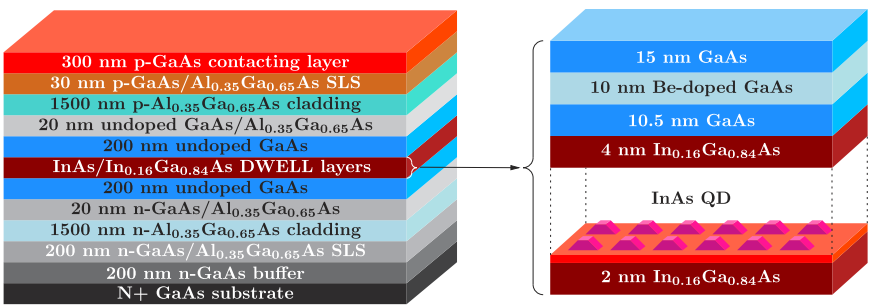

FIG. 1. Schematic of the layer composition for the co-doped devices whose gain and absorption are measured. The right-hand side shows an expanded view of a single DWELL layer and its spacer. The capping and spacer layers have been lifted away to better illustrate the position of the Si-doped dots.

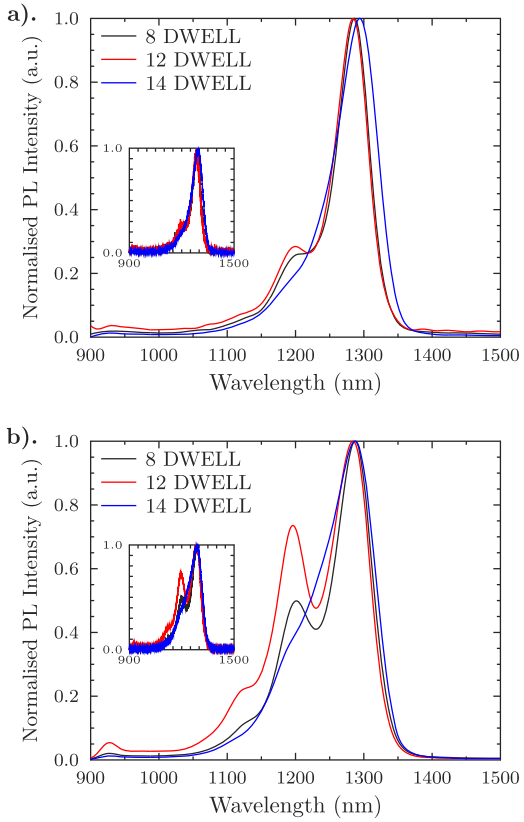

FIG. 2. Photoluminescence spectra for 8, 12, and 14 DWELL samples. Each plot includes filtered data and an inset showing the raw data. (a) Pumping power of 207.7 W cm^{-2}. (b) Pumping power of 2077 W cm^{-2}.

multi-section devices discussed in subsequent sections were selected from a region of the wafer where the GS peak position closely matched that of the other two samples.

III. MEASUREMENT

A. Experimental procedure

A typical multi-section device used for SCM measurements is shown in Fig. 3. The single-pass amplified spontaneous emission (ASE) spectra of a length of material can be measured by electrically pumping nominally identical sections that have a long passive section behind them; this passive section absorbs backward-traveling light, preventing reflection at the rear facet and ensuring that there is no round-trip amplification.

It can be shown that the net modal gain of the device depends on the ratio of the ASE spectra exiting the facet when two adjacent sections are pumped to that when a single section is pumped, as follows:[17]

$$G - \alpha_i = \frac{1}{L} \ln\left(\frac{I_{meas}(2L)}{I_{meas}(L)} - 1\right). \quad (1)$$

Here, I_{meas} is the measured intensity, G is the modal gain, and α_i is the internal optical mode loss.

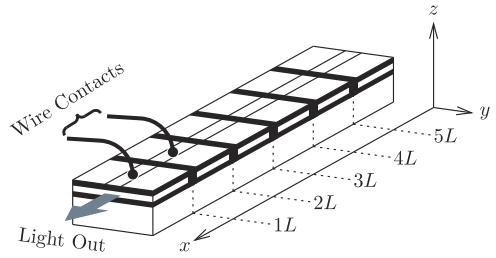

FIG. 3. Schematic of a typical broad area device used for segmented contact measurements with sections of length L.

Similarly, the net absorption, $A + \alpha_i$, can be found by measuring ASE from a single pumped section followed by pumping the section immediately behind it,

$$A + \alpha_i = \frac{1}{L} \ln\left(\frac{I^{(1)}_{meas}}{I^{(2)}_{meas}}\right), \quad (2)$$

where $I^{(1,2)}_{meas}$ correspond to the intensities measured from the front and back sections. To limit self-heating during the measurement, the devices were driven by a pulsed current source, with a pulse duration of 1 μs and a repetition frequency of 5 kHz.[22]

B. Analysis

An example set of spectra obtained using the method described above is plotted in Fig. 4. The net modal gain of the eight DWELL sample is plotted for several currents alongside the absorption spectrum. At long wavelengths, the spectra all converge to the same constant value. The PL spectra indicate that there are very few dot transitions in this region; however, it is possible to measure emission at these wavelengths due to the Coulomb interactions resulting from large carrier injection under the high-power PL conditions or under electrical injection. The absorption spectrum is a measurement of

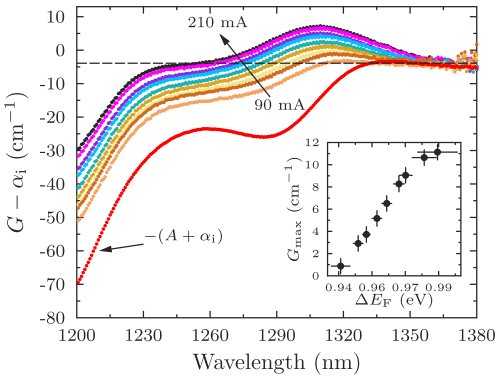

FIG. 4. The measured gain spectra for the sample with eight DWELL layers for a series of injected currents (steps of 15 mA). Two peaks are present in the gain spectra corresponding to ground-state and excited-state dot transitions. The absorption spectrum is also displayed (red markers). The inset displays the peak gain as a function of transparency energy.

the transitions in an unpumped section where there are minimal Coulomb interactions; consequently, in this long wavelength region, there are no or negligible dot states, meaning that the absorption here is negligible and the value of the constant is the internal mode loss α_i.

Positive gain is observed beyond the region where the absorption spectrum would indicate that the number of dot states is trivially low; this red shift is well documented and is attributed to the formation of excitons under high carrier injection. For sufficiently long wavelengths, there are very few dot states or excitons, meaning that the modal gain is zero and, therefore, the gain curves also converge to the internal mode loss. The internal mode losses obtained from the absorption spectra of each sample, plotted in Fig. 5, are collated in Table I. The peak in the absorption spectrum of the 14-layer DWELL sample is significantly broadened; this is consistent with the broadened dot distribution observed in Fig. 2.

Figure 5 shows that increasing the layer number generally increases the magnitude of the absorption, A; this is in line with expectations, as more DWELL layers means more total dot states, and the absorption spectra are a measure of the number of available transitions between valence and conduction states.

We next evaluate whether additional layers increase the gain in proportion to the increased layer number. If this is the case, it is unlikely that there are any significant differences in the carrier

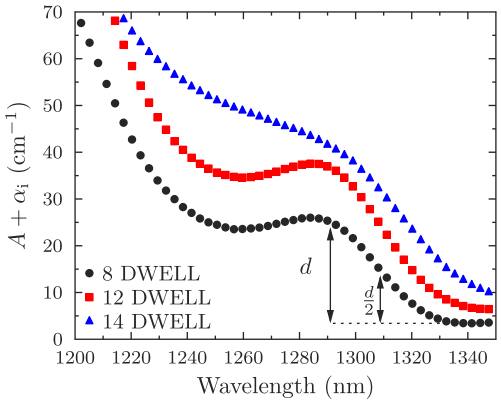

FIG. 5. The absorption spectra of each DWELL active region. Here, only every fourth data point is shown to enable the markers to be better distinguished. Also indicated is the position of the absorption edge, which we define to be the position of the minima in the second derivative corresponding to the longest wavelength absorption peak, and the position at which the value of the absorption is half that at the absorption edge.

TABLE I. The measured internal mode loss, α_i, for each of the samples alongside the internal mode loss per layer. The uncertainties presented here represent a one-sigma coverage interval.

Layer number	α_i (cm^{-1})	α_i (cm^{-1} layer^{-1})
8	3.9 ± 0.7	0.49 ± 0.09
12	6.3 ± 0.5	0.52 ± 0.04
14	8.5 ± 0.5	0.61 ± 0.04

population in the different layers. To isolate the effect of the number of DWELL layers on the laser performance, other potential differences between samples [e.g., differing Shockley–Read–Hall (SRH) recombination rates or different internal optical mode loss] must be removed. One way to do so is to compare the peak modal gain as a function of transparency energy;[9] this is the energy at which the rate of stimulated emission and the rate of absorption are both non-zero and coincide (i.e., $G = 0$), and it is, therefore, equal to the quasi-Fermi level separation (assuming that the carriers are well described by Fermi distributions), ΔE_F.[23] The quasi-Fermi level separation is closely related to the carrier concentration, making it a more intrinsic (effectively removing the effect of SRH recombination) comparison than, e.g., the device current.[24]

To determine the transparency energy for each curve, we found the wavelength at which the curve intersects a horizontal line with value $-\alpha_i$; this is illustrated by the dashed line in Fig. 4. The associated uncertainty was calculated using a Monte Carlo method[25] (MCM) to find the probabilistically symmetric, one-sigma (≈68 %) coverage interval by assigning the appropriate Gaussian distribution to measurements of α_i. The peak modal gain and associated one-sigma uncertainty were calculated simultaneously via the non-parametric Bootstrapping technique,[26] using the main MCM loop to calculate each resampling (with replacement). The maximum value of each resampling was recorded, and the best estimate for the peak gain was taken to be the mean of these values with the uncertainty given by the sample standard deviation.

An unintended consequence of using the transparency energy is that the results become dependent on the distribution of dot sizes within each sample. Inhomogeneity of dot sizes leads to broadening of spectral peaks because dots of different sizes have different spacing between energy levels and, therefore, emission/absorption characteristics. As such, the wider the distribution of sizes, the broader the gain peak. This is of importance here because broader gain spectra will intersect with the α_i line at shorter wavelengths and will, therefore, have comparatively larger transparency energies. This means that any difference in dot distributions between samples could lead to incorrect results. In fact, it has been shown that, even in the absence of size distribution, larger dots have broader spectra as their bound modes are more tightly spaced than smaller dots,[27] so even if the variance of sizes is the same between samples, differences in the mean could skew the results.

To reduce the effect of spectrum width, we have calculated a transition energy, $E_{transition}$, for each sample based on the width of the longest wavelength absorption peak. $E_{transition}$ is the energy at which the absolute magnitude of the absorption falls to half of the value at the absorption edge, as indicated in Fig. 5. The transition energies for the 8-, 12-, and 14-layer samples are 0.947, 0.945, and 0.939 eV, respectively. The difference between the transparency energy and the transition energy provides a measure of the carrier concentration, taking into account differences in dot distributions between samples.[28]

IV. RESULTS AND DISCUSSION

The results of completing the analysis described above for each sample are plotted in Fig. 6. Comparison of vertical uncertainties shown in Fig. 6 to those presented for α_i in the second column of Table I shows that the vertical uncertainty is dominated by the

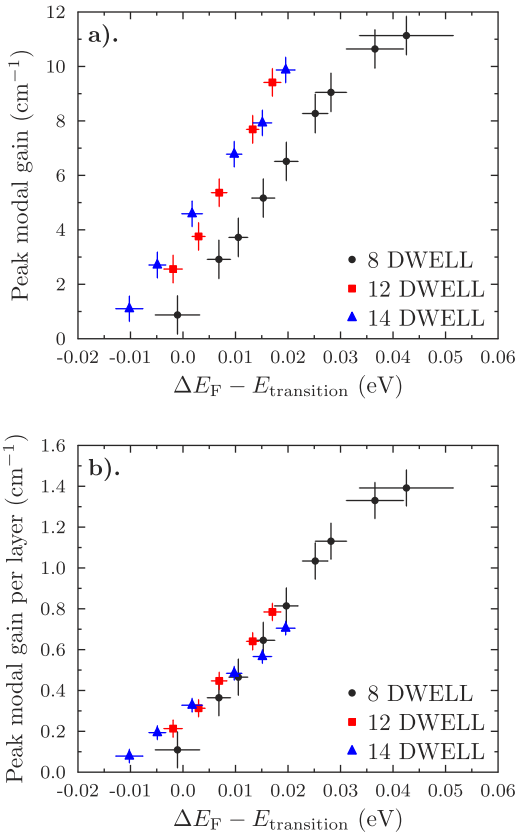

FIG. 6. (a) The measured peak modal gain of several DWELL samples plotted against the difference between the transparency energy and the transition energy. (b) The peak modal gain per layer for the same samples. We note that the vertical uncertainty is dominated by the uncertainty associated with determining α_i.

uncertainty in determining α_i. As such, the vertical uncertainty is largely systematic, and, therefore, the relative spacing of data points for the same sample is well determined.

The comparatively large horizontal uncertainties of the two points with the largest peak modal gain can be understood with reference to Fig. 4. The transparency points of the associated gain curves (210 and 195 mA) coincide with the shoulders of the curves, meaning that even small vertical perturbations of α_i lead to large changes in the horizontal placement of the transparency points.

Figure 6(a) shows that generally for the same carrier concentration, the greater the number of DWELL layers, the greater the peak modal gain. This is confirmed in Fig. 6(b), which demonstrates that even for thicker active regions, each layer contributes equally to the optical gain. This suggests that, within the range of layer numbers investigated here, neither uneven pumping nor optical overlap is an issue. We note, that the slope of the fourteen DWELL sample is comparatively shallow, leading to less peak gain at higher carrier densities. However, we do not believe that this is an intrinsic property of the number of layers, but rather that it is related to the broadening of the absorption edge shown in Figs. 2 and 5. At low carrier densities, a broad distribution results in more low-lying states that can contribute to the gain, whereas at higher carrier densities, a broader energy range of states is occupied, resulting in a lower peak modal gain. This is precisely the behavior shown in Fig. 6.

Table I shows that, within uncertainties, the internal mode loss per layer is consistent. This suggests that the internal optical mode loss comes from processes proportional to the layer number. A significant source of internal mode loss is the overlap of the optical mode with highly doped layers, resulting in free carrier absorption.[29] As discussed in Sec. II, these samples have p-dopants in the spacers between the DWELL layers, meaning that optical modes propagating through samples with more DWELL layers have a greater overlap with highly doped layers, which leads to increased internal mode loss.

The threshold condition for Fabry–Pérot (FP) lasers is

$$G - \alpha_i = \alpha_m, \tag{3}$$

where α_m is the distributed mirror loss.[30] The mirror losses should be independent of the number of DWELL layers. In addition, we have shown that active regions with more layers reach the same level of $G - \alpha_i$ at lower carrier densities, meaning that laser cavities with more layers will require a lower carrier density to reach threshold, and according to the discussion in Sec. I, they are likely to have better temperature insensitivity and longer laser lifetimes. However, for the doping levels used here, it can be inferred from Fig. 6(a) that the eight-layer sample produced the highest positive net gain. This is related to the fact that a greater range of carrier densities could be accessed. Samples with fewer layers have lower resistances; as such, when electrically pumped at the same power, samples with fewer layers will have a higher carrier density. In principle, a high power source would be able to access higher carrier densities and, therefore, higher net gain in the larger layer number samples; however, this is undesirable. Significantly increasing the power consumption of the device would mitigate the benefits associated with improved gain; however, there may be another way to improve the performance.

It is well known that the non-radiative recombination rate increases with modulation p-doping and that if the level of p-doping is too high, the increased current required outweighs the improved gain performance.[31] In the comparison here, samples with larger layer numbers have higher total p-doping, so this may be the origin of the lower layer number samples performing better.

In higher-layer-number samples, there is less need for the beneficial effects of p-doping with respect to higher gain. Hence, at higher layer numbers, a lower level of p-doping per layer would reduce the internal mode loss, improve radiative efficiency, and may allow higher net gains to be accessed without increasing the power of the electrical supply, leading to better overall performance.

V. SUMMARY

By comparing the gain spectra of structures with 8, 12, and 14 DWELL layers (which are nominally identical otherwise), we have presented two key findings:

1. At the same carrier concentration, the peak modal gain per layer is independent of the number of DWELL layers, indicating that there is no issue with optical overlap or unequal pumping of layers.
2. The internal mode loss per layer is almost independent of layer number, suggesting that the principal optical loss mechanism

is a layer-dependent process such as free-carrier absorption in the spacer layers, relating to p-doping.

Accordingly, active regions with more DWELL layers would require a lower carrier density to reach threshold, meaning that they are likely to be more temperature insensitive and have longer laser lifetimes. As high levels of p-dopants lead to increased free carrier absorption and non-radiative recombination, it is likely that the higher threshold currents of lasers with large DWELL numbers currently seen could be mitigated by reducing the amount of p-modulation doping.

ACKNOWLEDGMENTS

This work was supported by both the EPSRC Manufacturing Hub (Grant No. EP/Z532848/1) and the EPSRC Center for Doctoral Training in Compound Semiconductor Manufacturing (Grant No. EP/S024441/1). We also thank our colleagues at Cardiff University, Qiang Li, Balthazar Temu, and Zhao Yan, for their support with the PL measurement.

AUTHOR DECLARATIONS

Conflict of Interest

The authors have no conflicts to disclose.

Author Contributions

G. M. Jandu: Data curation (equal); Formal analysis (equal); Methodology (equal); Writing – original draft (equal); Writing – review & editing (equal). **A. R. Smith**: Methodology (equal); Writing – original draft (equal); Writing – review & editing (equal). **C. P. Allford**: Investigation (equal); Methodology (equal); Writing – review & editing (equal). **S. Power**: Resources (equal); Writing – review & editing (equal). **P. Mishra**: Writing – review & editing (equal). **Z. Cao**: Resources (equal); Writing – review & editing (equal). **L. Jarvis**: Methodology (equal); Writing – review & editing (equal). **X. Zhang**: Resources (equal); Writing – review & editing (equal). **H. Deng**: Resources (equal); Writing – review & editing (equal). **M. Tang**: Resources (equal); Writing – review & editing (equal). **H. Liu**: Resources (equal); Writing – review & editing (equal). **P. M. Smowton**: Conceptualization (equal); Supervision (equal); Writing – original draft (equal); Writing – review & editing (equal).

DATA AVAILABILITY

The data that support the findings of this study are openly available in the Cardiff University Research Data Repository https://doi.org/10.17035/cardiff.30293929, Ref. 32.

REFERENCES

[1] H. Deng *et al.*, J. Phys. D: Appl. Phys. **55**, 215105 (2022).
[2] V. S. Mikhrin, A. V. Zhabotinskii, M. S. Buyalo, S. V. Poltavtsev, S. S. Mikhrin, A. E. Gubenko, and A. R. Kovsh, in *2023 Optical Fiber Communications Conference and Exhibition (OFC)* (IEEE, 2023), pp. 1–3.
[3] T. Kageyama, K. Nishi, M. Yamaguchi, R. Mochida, Y. Maeda, K. Takemasa, Y. Tanaka, T. Yamamoto, M. Sugawara, and Y. Arakawa, in *2011 Conference on Lasers and Electro-Optics Europe and 12th European Quantum Electronics Conference (CLEO EUROPE/EQEC)* (Optica Publishing Group, 2011), p. 1. https://opg.optica.org/abstract.cfm?URI=CLEO_Europe-2011-PDA_1
[4] Z. Lv, S. Wang, S. Wang, H. Chai, L. Meng, X. Yang, and T. Yang, Opt. Express **31**(15), 24173 (2023).
[5] F. A. Al-Marhaby and M. S. Al-Ghamdi, Opt. Mater. **127**, 112191 (2022).
[6] G. Moreau, S. Azouigui, D.-Y. Cong, K. Merghem, A. Martinez, G. Patriarche, A. Ramdane, F. Lelarge, B. Rousseau, B. Dagens, F. Poingt, A. Accard, and F. Pommereau, Appl. Phys. Lett. **89**, 241123 (2006).
[7] P. M. Ilroy, A. Kurobe, and Y. Uematsu, IEEE J. Quantum Electron. **21**, 1958 (1985).
[8] P. M. Smowton, G. M. Lewis, A. Sobiesierski, P. Blood, J. Lutti, and S. Osbourne, Appl. Phys. Lett. **83**, 419 (2003).
[9] P. Blood, *Quantum Confined Laser Devices: Optical Gain and Recombination in Semiconductors* (Oxford University Press, 2015).
[10] B. Maglio, L. Jarvis, M. Tang *et al.*, Opt. Quantum Electron. **56**, 687 (2024).
[11] S. Saeed, M. Usman, S. Ali, L. Mustafa, I. Anjum, and J. Bashir, Physica B **683**, 415956 (2024).
[12] S. Shutts *et al.*, "Degradation of III–V quantum dot lasers grown directly on silicon substrates," IEEE J. Selec. Topics Quant. Electron. **25**(6), 1–6 (2019).
[13] P. Petroff and R. L. Hartman, Appl. Phys. Lett. **23**, 469 (1973).
[14] H. Deng, J.-S. Park, X. Yu, Z. Liu, H. Jia, H. Zeng, J. Yang, S. Pan, S. Chen, A. Seeds, M. Tang, P. Smowton, and H. Liu, Adv. Phys. Res. **3**, 2400045 (2024).
[15] P. M. Smowton, A. George, I. C. Sandall, M. Hopkinson, and H.-Y. Liu, IEEE J. Sel. Top. Quantum Electron. **14**, 1162 (2008).
[16] B. Maglio, L. Jarvis, C. P. Allford, S. Gillgrass, A. Enderson, S. Shutts, H. Deng, M. Tang, H. Liu, and P. M. Smowton, in *2022 IEEE Photonics Conference (IPC)* (IEEE, 2022), pp. 1–2.
[17] P. Blood, G. M. Lewis, P. M. Smowton, H. Summers, J. Thomson, and J. Lutti, IEEE J. Sel. Top. Quantum Electron. **9**, 1275 (2003).
[18] K. Y. Koichi Yamaguchi, K. Y. Kunihiko Yujobo, and T. K. Toshiyuki Kaizu, Jpn. J. Appl. Phys. **39**, L1245 (2000).
[19] P. Mishra *et al.*, "High temperature operation of Co-doped InAs quantum dot laser for O-band emission," IEEE Photon. J. **17**(3), 1–6 (2025).
[20] H. Y. Liu, D. T. Childs, T. J. Badcock, K. M. Groom, I. R. Sellers, M. Hopkinson, R. A. Hogg, D. J. Robbins, D. J. Mowbray, and M. S. Skolnick, IEEE Photonics Technol. Lett. **17**, 1139 (2005).
[21] N. Bart, C. Dangel, P. Zajac *et al.*, Nat. Commun. **13**, 1633 (2022).
[22] J.-S. Park, H. Deng, S. Pan, H. Wang, Y. Wang, J. Yuan, X. Zhang, H. Zeng, H. Jia, M. Dang, P. Mishra, G. Jandu, S. Chen, P. M. Smowton, A. Seeds, H. Liu, and M. Tang, J. Phys. D: Appl. Phys. **58**, 185101 (2025).
[23] M. G. A. Bernard and G. Duraffourg, Phys. Status Solidi B **1**, 699 (1961).
[24] P. M. Smowton, I. C. Sandall, H. Y. Liu, and M. Hopkinson, J. Appl. Phys. **101**, 013107 (2007).
[25] BIPM, IEC, IFCC, ILAC, ISO, IUPAC, IUPAP, and OIML,"Evaluation of measurement data—Supplement 1 to the 'Guide to the expression of uncertainty in measurement'—Propagation of distributions using a Monte Carlo method," Joint Committee for Guides in Metrology, JCGM 101, 2008.
[26] M. Klas, A. Trendowicz, Y. Ishigai, and H. Nakao, *In 2011 International Symposium on Empirical Software Engineering and Measurement* (IEEE, 2011), pp. 245–254.
[27] S. Guin and N. R. Das, in *2016 IEEE Region 10 Conference (TENCON)* (IEEE, 2016), pp. 3246–3248.
[28] Z. Li, S. Shutts, Y. Xue, W. Luo, K. M. Lau, and P. M. Smowton, Appl. Phys. Lett. **118**, 131101 (2021).

[29]L. Han, Z. Wang, N. Y. Gordeev, M. V. Maximov, X. Tang, A. A. Beckman, G. O. Kornyshov, A. S. Payusov, Y. M. Shernyakov, A. E. Zhukov, K. Li, R. Zhai, Z. Jia, H. Yang, and W. Zhang, Micromachines **14**, 1271 (2023).
[30]S. O. Slipchenko, A. A. Podoskin, N. A. Pikhtin *et al.*, "Analysis of threshold conditions for generation of a closed mode in a Fabry-Perot semiconductor laser," Semiconductors **45**, 663–667 (2011).
[31]R.-T. Liu, A.-T. Du, C.-F. Cao, J. Yang, J.-C. Wu, K. Wang, C. Yang, H. Huang, and Q. Gong, J. Appl. Phys. **136**, 223102 (2024).
[32]G. Jandu, A. Smith, C. Allford, L. Jarvis, S. Power, P. Mishra, Z. Cao, H. Huang, and M. Tang (2025), Data for "Optical gain in O-band active regions with multiple dot-in-well layers," Cardiff University Research Data Repository. https://doi.org/10.17035/cardiff.30293929